

ON THE USE OF DIGITAL IMAGE CORRELATION TO ANALYZE THE MECHANICAL PROPERTIES OF BRITTLE MATRIX COMPOSITES

François Hild, Jean-Noël Périé
Laboratoire de Mécanique et Technologie (LMT-Cachan)
ENS de Cachan / CNRS / Université Paris 6
61 avenue du Président Wilson
F-94235 Cachan Cedex, France

Jacques Lamon and Matthieu Puyo-Pain
Laboratoire des Composites Thermostructuraux (LCTS)
UMR 5801 CNRS / Snecma / CEA / Université Bordeaux 1
3 allée de La Boétie
F-33600 Pessac, France

ABSTRACT

The 2D digital image correlation technique needs a single CCD camera to acquire the surface patterns of a region of a specimen in the undeformed and deformed states. With two images, one can determine in-plane displacement and strain fields. Its performance is assessed and discussed in real experimental situations. Thanks to its sub-pixel resolution, it can be used to monitor experiments even for brittle and quasi-brittle materials, namely materials for which the strain levels remain low (less than 0.1% in many cases). Two examples are given. Firstly, elastic properties of BraSiC (a silicon-based braze to assemble SiC/SiC composites) are extracted from kinematic fields estimated by utilizing a digital image correlation method. Secondly, the technique is utilized to analyze experimental results of a plane shear experiment and validate a damage model describing different degradations in a C/C composite material.

INTRODUCTION

The prediction of the mechanical behavior of structures is performed through numerical computations based on constitutive equations. The parameter tuning is often performed by using classical (and homogeneous) mechanical tests. The current development of reliable full-field measurement techniques¹ allows for a better characterization of the complex behavior of heterogeneous materials and the non-uniform response of structures to external loads. Full-field measurements can be used in a variety of ways, namely:

- to monitor in-service structures and weak zones therein (e.g., airplanes, bridges, buildings);
- to check boundary conditions before performing the mechanical test itself.² In that case, it allows the experimentalist to control whether the boundary conditions correspond to the desired ones;
- to control an experiment^{3,4} by using optical means as opposed to gauges or extensometers;
- to perform heterogeneous tests for which single measurements (e.g., by strain gauges, extensometers, clip gauges) are not sufficient to fully analyze an experiment, and particularly when the spatial heterogeneity is not known *a priori* (e.g., damage localization⁵ as shown below);

- to study an experiment by using contactless techniques. This provides useful solutions to aggressive, hot, corrosive environments, or very soft solids⁶ for which gauges are not adapted;
- to identify material properties as discussed below for a ceramic-based braze that can be used to joint ceramics of ceramic-matrix composites. Different strategies can be followed⁷. In the present case, FE updating is used to determine elastic properties of BraSiC from displacement fields estimated by utilizing a digital image correlation method;
- to propose damage and failure scenarios by using damage and fracture models as shown below for the analysis of a shear experiment on a C/C composite.

DIGITAL IMAGE CORRELATION

The full-field measurement technique used herein is digital image correlation^{1,8,9} that has proven to be an efficient, robust and affordable tool. Resolution of the technique can be extended much below the pixel value even at microscopic scales¹⁰⁻¹² to determine mechanical properties of materials. By using a CCD camera, pictures at different stages are recorded during the test. The specimen is usually coated by a random black and white pattern (e.g., the second example). Sometimes the natural texture of the observed surface is sufficient to use the technique with no coating (see first example). The in-plane displacement map is computed with a correlation technique between an initial picture and a subsequent one.

Principle of Image Correlation

One considers a sequence of sub-images (i.e., a square region) that will be referred to as zone of interest (ZOI). The aim of correlation method is to match the zone of interest in the two images (Fig. 1).

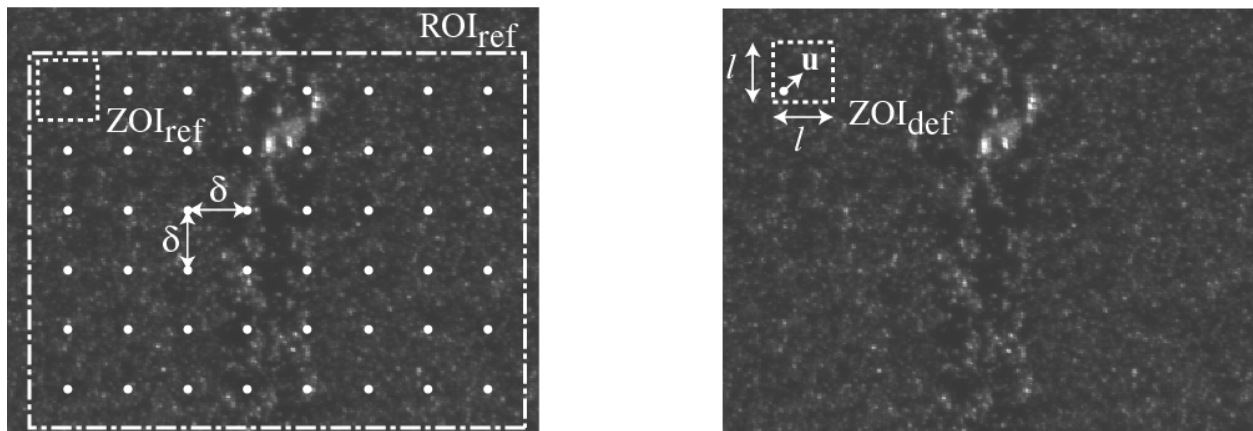


Figure 1. Schematic diagram showing the correlation parameters in a reference picture (left) and a picture in the deformed state (right).

The displacement of one ZOI with respect to the other one is a two-dimensional shift of an intensity signal digitized by a CCD camera. To estimate a shift between two images, one of the standard approaches utilizes a correlation function. One considers signals $g(\mathbf{x})$ that are merely perturbations of a shifted copy $f(\mathbf{x}-\mathbf{u})$ of some reference signal $f(\mathbf{x})$

$$g(\mathbf{x}) = f(\mathbf{x}-\mathbf{u}) + b(\mathbf{x}) \quad (1)$$

where \mathbf{u} is the unknown displacement and $b(\mathbf{x})$ a random noise. To evaluate the shift \mathbf{u} , one may minimize the norm of the difference between $f(\mathbf{x}-\mathbf{v})$ and $g(\mathbf{x})$ with respect to x and y

$$\min_{\mathbf{v}} \|g - f(\cdot-\mathbf{v})\|^2. \quad (2)$$

If one chooses the usual quadratic norm $\|f\|^2 = \iint f(\mathbf{x})^2 dx$, the previous minimization is equivalent to maximizing

$$h(\mathbf{v}) = (g \otimes f)(\mathbf{v}) = \iint g(\mathbf{x})f(\mathbf{x}-\mathbf{v}) dx \quad (3)$$

where \otimes denotes the cross-correlation operator. Furthermore, when b is a white noise, the previous estimate is optimal. The computation of a cross-correlation can be performed either in the original space^{9,13} or in the Fourier space,¹⁴⁻¹⁶ by using fast Fourier transforms (FFT)

$$g \otimes f = \text{FFT}^{-1} (\text{FFT}[g] \overline{\text{FFT}[f]}) \quad (4)$$

where the complex conjugate is overlined.

Correlation Algorithm for Digital Images

Two images are considered. The first one, referred to as ‘reference image’ and the second one, called ‘deformed image.’ One extracts the largest value p of a region of interest (ROI) of size $2^p \times 2^p$ pixels centered in the reference image. The same ROI is considered in the deformed image. A first FFT correlation is performed to determine the average displacement \mathbf{U}_0 of the deformed image with respect to the reference image. This displacement is expressed in an integer number of pixels and is obtained as the maximum of the cross-correlation function evaluated for each pixel of the ROI. This first prediction enables one to determine the maximum number of pixels that belong to the two images. The ROI in the deformed image is now centered at a point corresponding to displaced center of the ROI in the reference image by an amount \mathbf{U}_0 .

The user usually chooses the size of the zones of interest (ZOI) by setting the value of l so that the size is $2^s \times 2^s$ pixels. To map the whole image, the second parameter to choose is the separation δ between two consecutive ZOI: $1 \leq \delta \leq l = 2^s$ pixels. The latter defines the mesh formed by the centers of each ZOI used to analyze the displacement field (Fig. 1). The following analysis is performed for each ZOI independently. A first FFT correlation is carried out and a first value of the in-plane displacement correction $\Delta\mathbf{U}$ is obtained. The value $\Delta\mathbf{U}$ is again integer numbers so that the ZOI in the deformed image can be displaced by an additional amount $\Delta\mathbf{U}$. The displacement residues are now less than 1/2 pixel in each direction. A sub-pixel iterative scheme can be used. A new cross-correlation is performed. A sub-pixel correction of the displacement $\delta\mathbf{U}$ is obtained by determining the maximum of a parabolic interpolation of the correlation function. The interpolation is performed by considering the maximum pixel and its

eight nearest neighbors. Therefore, one obtains a *sub-pixel* value. By using the ‘shift/modulation’ property of the Fourier transform, one can move the windowed ZOI in the deformed image by an amount δU . Since an interpolation was used, one may induce some errors requiring to re-iterate by considering the new ZOI until a convergence criterion is reached. The criterion checks whether the maximum of the interpolated correlation function increases as the number of iteration increases. Otherwise, the iteration scheme is stopped. The procedure, $CORRELI^{LMT,6}$, is used to measure local displacements and then extract strain fields.

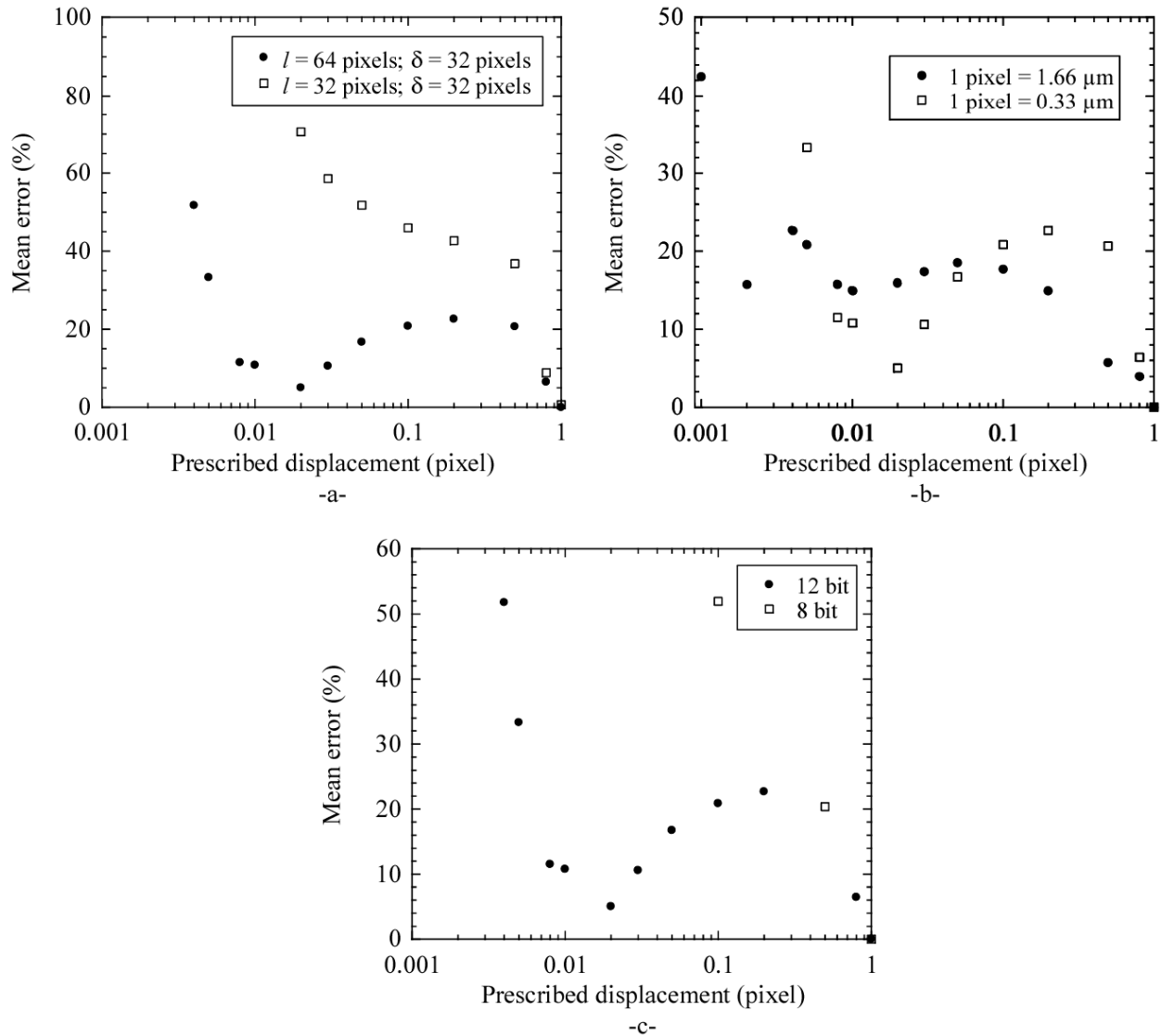


Figure 2. Performance in terms of mean error vs. prescribed displacement for different correlation parameters (a), magnifications (b) and digitizations (c).

Several experiments are performed to evaluate the resolution and quality of the system. Images of the surface of the materials are numerically shifted by a constant displacement value. The resulting average determined by the DIC system, and the prescribed displacement are compared. The corresponding errors are plotted in Fig. 2. The error is evaluated for two different ZOI sizes. One can note that a ZOI size increase reduces the measured displacement error, but

also reduces the number of independent measurements. The displacement resolution for the DIC system was found to be 10^{-2} pixel when an error of about 20 % is allowed for two analyzed magnifications. This result is obtained for a 12-bit image of the texture whereas it is much higher for the same texture with an 8-bit digitization.

Furthermore, successive images were taken under three different experimental conditions of a specimen that was subject to a constant load, to determine the standard strain uncertainty σ_ϵ induced by the system at various magnifications and for different gauge sizes ($L_x = L_y$). It is worth pointing out that σ_ϵ is 7.8×10^{-5} at a magnification of 1 pixel = $0.33 \mu\text{m}$ for a gauge length of 128 pixels. The larger the gauge length (i.e., spatial resolution), the smaller the uncertainty as depicted by a power law trend (solid line in Fig. 3).

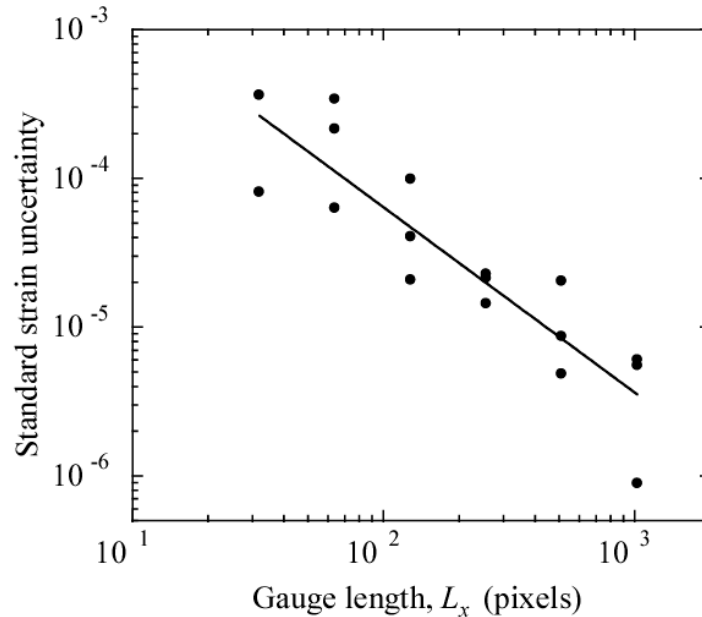


Figure 3. Standard strain uncertainty for different gauge sizes when $l = 64$ pixels and $\delta = 32$ pixels. The straight line shows a power law fit with an exponent of -1.25 .

IDENTIFICATION OF ELASTIC PROPERTIES OF A BRAZE JOINT

Joining materials, whose difficulty and cost of manufacturing complex shape is prohibitive, is a common technique to make structures from simple elements.¹⁷⁻¹⁹ In the typical case of ceramics and ceramic-matrix composites that operate under severe conditions of temperature and environment, ceramic-based adhesives are required so that the latter must not be the performance-limiting link in the assembled body.²⁰⁻²³ In the present study, the BraSiC process is chosen to join silicon carbide parts. The BraSiC joint is a silicon-based joint and the BraSiC process is a non-reactive brazing so that no interphase is created between the joint and SiC or SiC/SiC substrates.^{24,25} Mechanical and thermal properties of ceramic parts are therefore unaltered. Data on the mechanical behavior and properties of joints are a prerequisite to the design of reliable parts.²⁶⁻²⁸ The identification of joint properties is difficult because of its size (about $100 \mu\text{m}$ in the present case, Fig. 4a) and because BraSiC bulk samples cannot be made. Consequently, mechanical properties of the joint must be measured *in situ*.

The samples analyzed hereafter are made of α -SiC bars provided by Boostec Inc. The elastic properties of SiC are $E_{\text{SiC}} = 420 \text{ GPa}$ and $\nu_{\text{SiC}} = 0.14$. They are taken from a larger plate of silicon carbide whose dimensions are $100 \times 150 \times 8 \text{ mm}^3$. Dimensions of samples are $100 \times 7.5 \times 6.1 \text{ mm}^3$. The width of the joint is $85 \pm 5 \mu\text{m}$. One face of the specimen is carefully polished to reveal heterogeneities and porosities of the joined material to meet optical requirements. The gray level distribution should be as wide as possible to use the full dynamic range of the digital camera. However, it appeared that the difference in reflection induced by SiC and BraSiC can alter the distributions in gray levels (Fig. 4a) and therefore affects the results. The gray level distribution of a digital image of the surface of the material taken next to the joint exhibits a lot of noise that is detrimental to a good correlation. To increase the quality of images (i.e., to improve the distribution of gray level by homogenizing the image contrast), the surface of the samples was lightened by using a grazing beam (Fig. 4b).²⁹

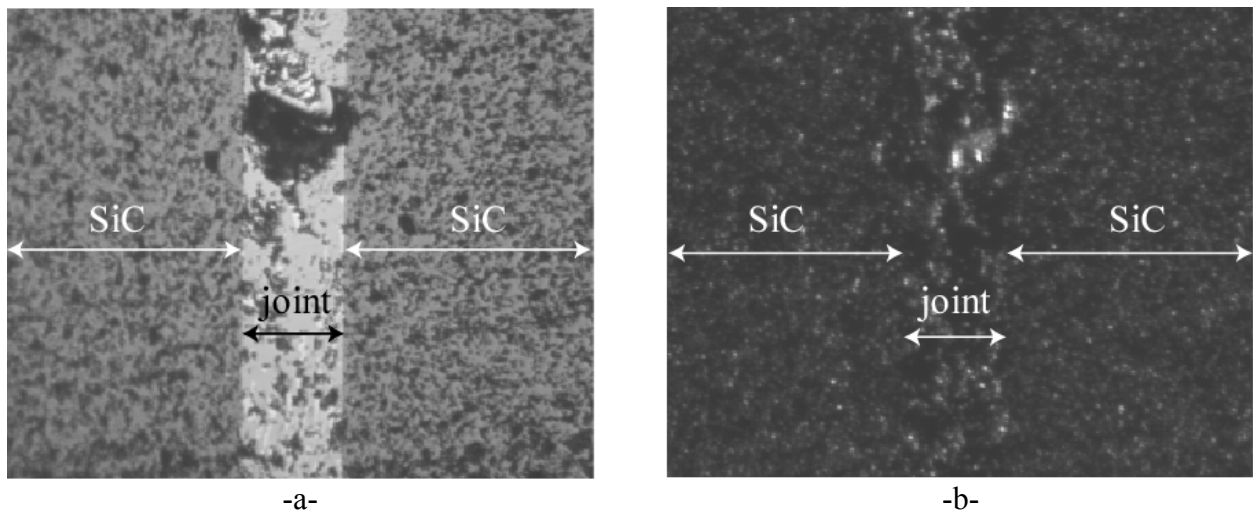


Figure 4. Digital images (1280×1024 pixels, 1 pixel = $0.33 \mu\text{m}$) acquired with a normal lighting beam (a) and a grazing lighting beam (b).

An optical microscope was mounted on the testing machine with a 12-bit digital camera (Fig. 5). Images of the specimen surfaces are taken at various loading steps. The optical microscope monitors the SiC substrate and the joint at various scales.

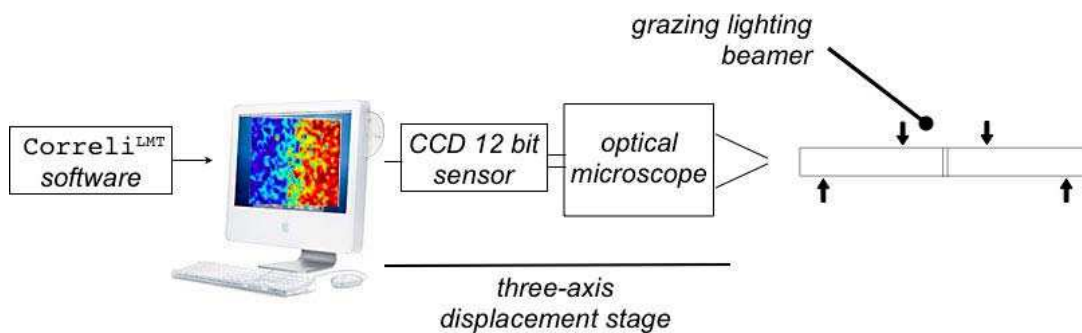


Figure 5. Schematic of the testing procedure using a DIC technique.

The description of strain and stress states in the joint is not straightforward. Finite element computations are then used to estimate the elastic constants from displacement field measurements. The finite element computations are carried out for two dimensional plane stress conditions using the MSC.Marc 2000 finite element code. A refined 3-node element mesh is used in the joint area. The elastic constants of the SiC substrates are known. The zone referred to as ROI* is identical to the experimental ROI (Fig. 6). The finite element mesh coincides exactly with the correlation grid. Joint elastic constants correspond to the minimum of J_{4B} that represents the deviation between experimental and computed displacement fields in (x,y) coordinates of correlation measurement points and FE nodes

$$J_{4B}(E_{\text{joint}}, \nu_{\text{joint}}) = \sum_F \sum_{\{x,y\}} \left[\tilde{U}_{\text{exp}}(x, y, F) - \tilde{U}_{\text{FEM}}\left(x, y, F, \frac{E_{\text{joint}}}{E_{\text{SiC}}}, \nu_{\text{joint}}, \nu_{\text{SiC}}\right) \right]^2 \quad (5)$$

where \tilde{U} is the displacement vector from which the rigid body motion is subtracted. The elastic properties E_{joint} and ν_{joint} are determined by seeking the minimum of J_{4B} .

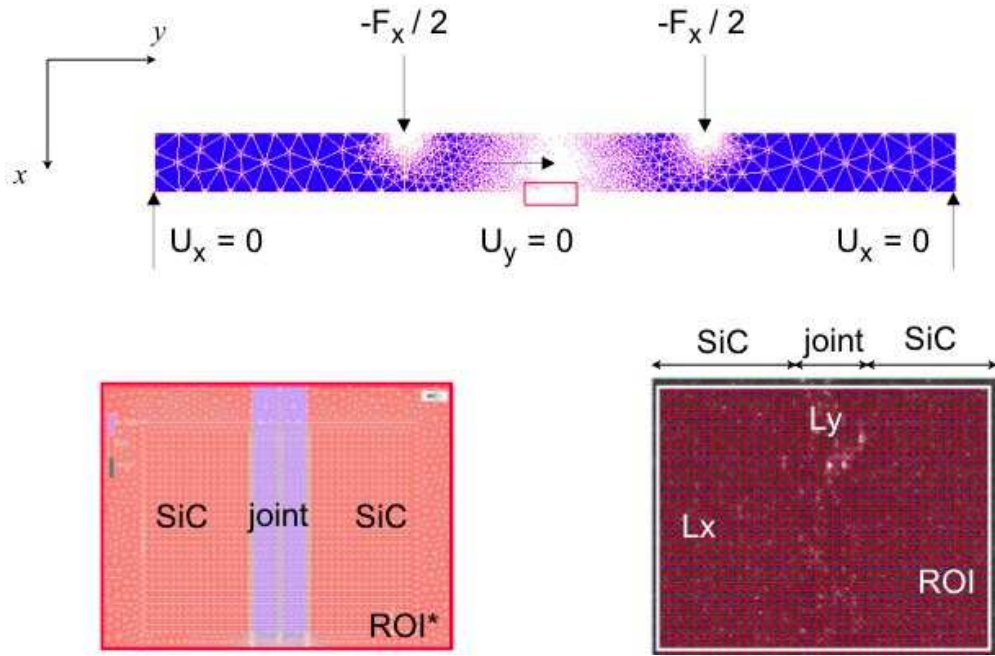


Figure 6. Identification method in four-point bending.

A computation is carried out and J_{4B} is evaluated. Only the J_{4By} components could be considered for the determination of E_{joint} and ν_{joint} , since U_x displacements cannot be measured accurately. Even for the maximum load level, U_x displacements do not exceed 0.03 pixel, which is of the order of the uncertainty and resolution, whereas U_y displacements are much greater and reach 0.1 pixel (see Fig. 7). By minimizing J_{4By} , the values $E_{\text{joint}} = 166 \pm 35$ GPa and $\nu_{\text{joint}} = 0.43 \pm 0.05$ can be identified. These estimates are comparable to the reduced modulus determined by nanoindentation tests carried out on the same sample.²⁹